



Resonance assignment of the outer membrane protein AlkL in lipid bilayers by proton-detected solid-state NMR

Tobias Schubeis¹ · Tom S. Schwarzer² · Tanguy Le Marchand¹ · Jan Stanek¹ · Kumar Tekwani Movellan³ · Kathrin Castiglione^{2,4} · Guido Pintacuda¹ · Loren B. Andreas^{1,3}

Received: 16 April 2020 / Accepted: 19 June 2020 / Published online: 30 June 2020
© Springer Nature B.V. 2020

Abstract

Most commonly small outer membrane proteins, possessing between 8 and 12 β -strands, are not involved in transport but fulfill diverse functions such as cell adhesion or binding of ligands. An intriguing exception are the 8-stranded β -barrel proteins of the OmpW family, which are implicated in the transport of small molecules. A representative example is AlkL from *Pseudomonas putida* *GPOI*, which functions as a passive importer of hydrophobic molecules. This role is of high interest with respect to both fundamental biological understanding and industrial applications in biocatalysis, since this protein is frequently utilized in biotransformation of alkanes. While the transport function of AlkL is generally accepted, a controversy in the transport mechanism still exists. In order to address this, we are pursuing a structural study of recombinantly produced AlkL reconstituted in lipid bilayers using solid-state NMR spectroscopy. In this manuscript we present ¹H, ¹³C and ¹⁵N chemical shift assignments obtained via a suite of 3D experiments employing high magnetic fields (1 GHz and 800 MHz) and the latest magic-angle spinning (MAS) approaches at fast (60–111) kHz rates. We additionally analyze the secondary structure prediction in comparison with those of published structures of homologous proteins.

Keywords ¹H-detected solid-state NMR · Membrane proteins · Lipid bilayers · Alkane transport · Beta-barrel

Abbreviations

IMAC Immobilized metal affinity chromatography
EDTA Ethylenediaminetetraacetic acid
LDAO Lauryldimethylamine N-oxide

OG N-octyl- β -D-glucopyranoside
DMPC 1,2-Dimyristoyl-sn-glycero-3-phosphocholine
CP Cross polarization
INEPT Insensitive nuclei enhanced by polarization transfer
BASS-SD Band-selective spectral spin diffusion
TOCSY Total correlation spectroscopy
MAS Magic-angle spinning

Electronic supplementary material The online version of this article (<https://doi.org/10.1007/s12104-020-09964-5>) contains supplementary material, which is available to authorized users.

✉ Guido Pintacuda
guido.pintacuda@ens-lyon.fr

✉ Loren B. Andreas
land@nmr.mpibpc.mpg.de

¹ Centre de RMN à Très Hauts Champs de Lyon (FRE 2034 - CNRS, UCB Lyon 1, ENS Lyon), Université de Lyon, 5 rue de la Doua, 69100 Villeurbanne, France

² Institute of Biochemical Engineering, Technical University of Munich, Boltzmannstraße 15, 85748 Garching, Germany

³ Department for NMR-Based Structural Biology, Max Planck Institute for Biophysical Chemistry, Am Faßberg 11, 37077 Göttingen, Germany

⁴ Present Address: Institute of Bioprocess Engineering, FAU Erlangen-Nürnberg, Paul-Gordan Str. 3, 91052 Erlangen, Germany

Biological Context

Due to the ability to specifically degrade alkanes, the hydroxylase (Alk) system of bacteria such as *Pseudomonas putida* *GPOI* is of potential interest for the chemical industry in terms of biocatalysis and may even find applications in bioremediation of crude oil pollutions (Meng et al. 2018). The catalytic complex is located at the cytoplasmic membrane consisting of AlkB, an integral-membrane non-heme diiron monooxygenase, the rubredoxin AlkG and the rubredoxin reductase AlkT (van Beilen et al. 2002; van Beilen and Funhoff 2007). These proteins efficiently convert linear alkanes to primary alcohols when in isolation but showed

only very limited turnover when engineered into *Escherichia coli* (Chen 2007). This suggests the crucial role of the outer membrane protein AlkL for uptake of medium to long chain alkanes, which are not capable to diffuse through the highly hydrophilic lipopolysaccharide layer at the outer membrane. Indeed, coexpression of AlkL significantly improves whole-cell based hydroxylation of various hydrophobic molecules (Julsing et al. 2012; Hsieh et al. 2018; van Nuland et al. 2016).

AlkL is counted into the family of OmpW proteins and structures of homologs such as *E. coli* OmpW (sequence identity 24%) and *Pseudomonas aeruginosa* OprG (sequence identity 22%) have already been solved by X-ray crystallography and solution NMR spectroscopy (Hong et al. 2006; Touw et al. 2010; Horst et al. 2014; Kucharska et al. 2015). Interestingly, the crystal and NMR structures show a consistent 8-stranded elliptical β -barrel but significant differences in the extracellular loops, namely β -sheets that extend beyond the hydrophobic membrane interior in crystals and long flexible loops in solution. Diffusion of small hydrophobic molecules through a lateral opening into the membrane was suggested as a transport mechanism of OmpW (Hong et al. 2006). Due to the increased flexibility in solution, the previous NMR studies were not entirely supportive to this model. One might argue that loops are stabilized by crystal packing or that detergents destabilize the loop structure in solution, what remains evident is the importance of dynamics of the extracellular regions in OmpW proteins.

Here we report the chemical shift assignments of AlkL in DMPC lipid bilayers obtained by ^1H -detected solid-state NMR. The use of a fully protonated sample and magic-angle spinning above 100 kHz allowed the combined use of amide-proton and alpha-proton detected spectra for backbone assignment as well as extensive assignment of side-chain ^{13}C and ^1H resonances. The lipid environment closely resembles the native membrane and with this sample formulation we anticipate reliable insights into structure and function of AlkL.

Methods and experiments

Protein expression and purification; sample preparation

AlkL (28–230) from *P. putida* GPo1 (Uniprot Q00595) was expressed with a short C-terminal linker and a His-8 tag (in total 219 residues) and purified essentially as described previously (Schwarzer et al. 2017). Uniform ^{13}C and ^{15}N isotope labeling was achieved by the use of M9 minimal media containing 3 g/L ^{13}C -glucose and 1 g/L $^{15}\text{NH}_4\text{Cl}$. Deuterated glucose and D_2O based media were used for ^2H , ^{13}C , ^{15}N -labelled samples. AlkL was extracted from inclusion

bodies and purified by IMAC in 50 mM Tris/HCl pH 8, 500 mM NaCl, 20–500 mM imidazole, 10% glycerol, 6 M guanidine HCl and refolded by drop-wise rapid dilution into 20 mM Tris/HCl pH 8, 1 mM EDTA, 1 M Urea, 2% LDAO. The refolded protein was further purified by anion exchange chromatography in 10 mM TRIS/HCl pH 8, 20–300 mM NaCl, 0.05% LDAO. The buffer was then exchanged to 20 mM phosphate pH 7, 2% OG using a desalting column. Protein concentrations were estimated based upon the absorption at 280 nm using a molar extinction coefficient of $34,380 \text{ M}^{-1} \text{ cm}^{-1}$. DMPC in 1% OG was added to achieve a protein to lipid ratio of 2:1, and the detergent was removed by dialysis against 20 mM phosphate buffer pH 7 using a 20 kDa cutoff membrane. After 2 days the white precipitate was collected by centrifugation, washed with buffer and packed into either 1.3 mm (deuterated sample) or 0.7 mm (protonated sample) MAS rotors using an ultracentrifuge packing device (Giotto Biotech).

Solid-state NMR spectroscopy

NMR spectra were recorded using a 0.7 mm triple-resonance (^1H , ^{13}C , ^{15}N) probe on a 1000 MHz Bruker Avance III spectrometer or using a 1.3 mm triple-resonance (^1H , ^{13}C , ^{15}N) probe on a 800 MHz spectrometer. All data were recorded at the MAS frequency of 111 kHz (0.7 mm probe) or 55 to 60 kHz (1.3 mm probe). The temperature of VT nitrogen gas was regulated to maintain a sample temperature of about 310 K. Backbone and sidechain resonance assignments were obtained from a set of three dimensional NMR spectra (Barbet-Massin 2014; Stanek 2016). Experimental details are given in table S1 and S2. Adamantane was used as the external reference. Spectra were processed using TopSpin 3.5 (Bruker Biospin) or NMRpipe (Delaglio et al. 1995) by zero filling to double the number of time increments, and apodization with a squared shifted cosine function (SSB 2 to 3). The direct dimension (^1H) acquisition time was truncated to 8 ms. Spectral analysis and assignment was accomplished with CcpNmr Analysis (Vranken 2005) and Sparky (Lee et al. 2015). The signal to noise ratio was estimated from a 1D hNH spectrum with 20 ms acquisition time, processed with 20 Hz exponential line broadening.

Sequence alignment and secondary structure analysis

Sequence alignment was performed with the Clustal Omega (Sievers, et al. 2011) implementation on the Uniprot server using entries Q00595 (AlkL), P0A915 (OmpW) and Q9HWW1 (OprG). Secondary structure elements of AlkL were predicted from the assigned chemical shifts using TALOS-N (Shen and Bax 2013). Deposited chemical shifts of OmpW (BMRB Entry 19,637) and OprG (BMRB Entry

25,768) were reanalyzed using TALOS-N as well. Secondary structure elements of X-ray structures were directly transferred from the respective PDB entries (2F1T and 2X27).

Extent of assignments and data deposition

AlkL was expressed by *E. coli* into inclusion bodies and purified under denaturing conditions followed by refolding into detergent micelles. Denaturation ensured the efficient back exchange of amide protons for the deuterated samples. The refolding efficiency was evaluated from the heat-modifiability of AlkL in SDS-PAGE (Fig. 1a). Folded AlkL is denatured inefficiently by SDS at room temperature and migrates differently than the unfolded protein. We estimated the refolding efficiency to > 90%. The yield of ^{13}C , ^{15}N and ^2H , ^{13}C , ^{15}N -labeled protein after purification and refolding was about 20 and 10 mg per liter of culture, respectively. Several types of lipids and different lipid to protein ratios were tested initially with ^{15}N -labeled AlkL as described in (Schubeis et al. 2018). Lipids were saturated with OG detergent, initially forming mixed micelles. Removal of OG by dialysis resulted in the formation of multilamellar vesicles, which appear as a white precipitate. A transmission electron micrograph of the final NMR sample is shown in Fig. 1b. The precipitated vesicles were ultracentrifuged into MAS NMR rotors.

The 2D ^1H - ^{15}N spectrum of deuterated and protonated AlkL are shown in Fig. 2a,b. The protonated sample showed an average ^1H linewidth of 150 Hz at 111 kHz MAS, the deuterated sample 90 Hz at 111 kHz MAS and 120 Hz at 60 kHz MAS. As concluded elsewhere before, deuteration is

still beneficial for ^1H linewidth and coherence lifetimes, even at > 100 kHz MAS (Xue, et al. 2017; Cala-De Paepe et al. 2017). Even though the fully protonated sample showed a lower resolution most assignments were made on this sample. While a deuterated sample only permits the classic set of $^1\text{H}^{\text{N}}$ -detected triple-correlation spectra for backbone sequential assignment, it was useful in assigning loop residues for which peak intensities were lower. Fully protonated samples allow recording of an additional set of $^1\text{H}\alpha$ -detected spectra, which exploit the favorable resolution of the 2D $\text{C}\alpha$ - $\text{H}\alpha$ fingerprint. The $^{13}\text{C}\alpha$ region of 2D ^1H - ^{13}C correlation spectra of AlkL, reconstituted in DMPC, is shown in Fig. 2c. α -protons also display ^1H linewidth of approximately 150 Hz, which is in line with non-crystalline membrane protein samples studied previously and indicative for high sample homogeneity (Lalli 2017; Lakomek et al. 2017). The decent signal to noise ratio ($S/N/\sqrt{t}=24.7$) and long refocused transverse coherence lifetimes (T_2^*) of 3.6 ms ($^1\text{H}^{\text{N}}$), 18 ms (^{15}N), 12.2 ms ($^{13}\text{C}\alpha$) and 17 ms ($^{13}\text{C}'$) obtained for the sample at 110 kHz allowed the acquisition of an extensive set of three dimensional spectra. The combination of amide and α -proton detected spectra proved to be very powerful for sequence specific resonance assignment. While in the classic amide-based backbone walk both the $^1\text{H}^{\text{N}}$ and ^{15}N chemical shift of a pre/succeeding residue needs to be identified, the $^1\text{H}\alpha$ detected spectra add the sequential ^{15}N chemical shift, facilitating the linkage dramatically. The strategy relies on the identification of $^1\text{H}^{\text{N}}$, $^1\text{H}\alpha$, $^{13}\text{C}\alpha$ and ^{15}N resonances of individual spin-systems (i.e. intraresidue correlations) which is, fortunately, often straightforward, using the hCANH and hNCAH spectra as demonstrated in Fig. 2d. The spectra in Fig. 2d were acquired simultaneously to improve sensitivity and maximize consistency of chemical shifts (Stanek et al. 2020; Sharma et al. 2020). The succeeding $^{15}\text{N}(i+1)$ chemical shift can then be found in the hNcoCAH spectrum and adjacent residues are simply linked over the $^{13}\text{C}\alpha$ resonance. Additional $^{13}\text{C}'$ and $^{13}\text{C}\beta$ correlations resolved most of remaining ambiguities, finally resulting in backbone assignments of 172 (out of 219) residues, corresponding to 79% total and more than 90% of the detectable residues. An overview of assigned heteronuclei is provided in figure S2. Most unassigned residues are located at the N- and C-termini and in the region between residues 33 and 53. These fragments likely show increased dynamics and are therefore undetectable in the CP-based MAS spectra. In general, the highest peak intensity was observed in the transmembrane β -strands, while the loop regions were more challenging to assign due to lower signal intensity. The automated assignment algorithm FLYA was employed to jointly analyze the large set of correlation spectra and already identified the transmembrane β -strands. Manual analysis was necessary to extend these assignments into loop residues. High sensitivity data, recorded on a deuterated sample in a larger 1.3 mm

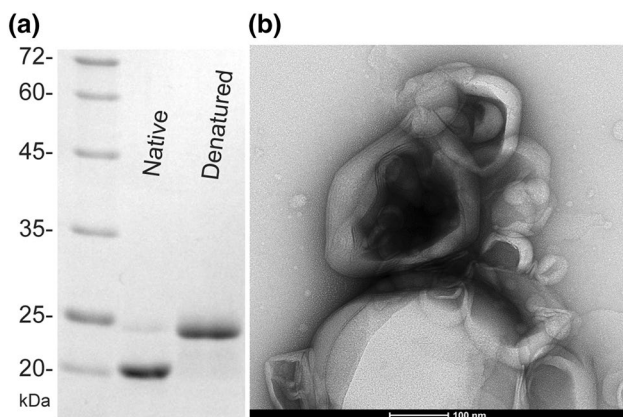


Fig. 1 **a** SDS-PAGE analysis of purity and folding of AlkL. Folded (Native) sample was incubated with SDS-sample buffer at room temperature; the denatured sample was heated to 95 deg. **c** **b** Transmission electron micrographs of multilamellar vesicle preparations containing AlkL

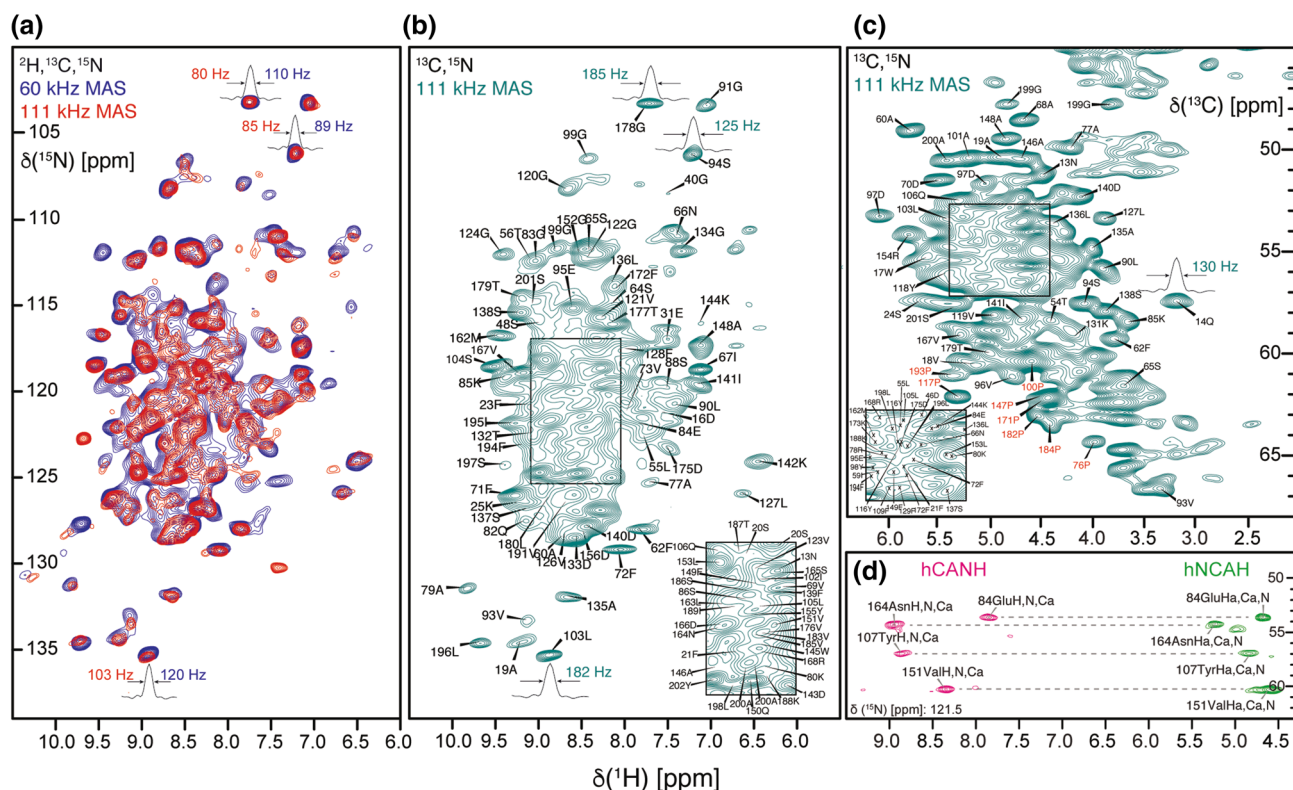


Fig. 2 **a** 2D ^1H - ^{15}N correlation spectra (hNH) of ^2H (100% ^{15}N), ^{13}C , ^{15}N -labeled AlkL in DMPC vesicles recorded on a sample packed in a 1.3 mm rotor with 60 kHz MAS (blue) or in a 0.7 mm rotor with 111 kHz MAS on a 1 GHz spectrometer. **b** hNH spectrum of fully protonated ^{13}C , ^{15}N -labeled AlkL recorded with 111 kHz MAS. **c** $^{13}\text{C}\alpha$ - $^{1}\text{H}\alpha$ region of 2D ^1H - ^{13}C correlation spectrum (hCH)

of fully protonated ^{13}C , ^{15}N labeled AlkL recorded with 111 kHz MAS. **d** Slice of two 3D ^1H - ^{13}C - ^{15}N correlation spectra (hCANH and hNCAH) at the ^{15}N frequency of 121.5 ppm. The spectra were recorded simultaneously on fully protonated AlkL. Sequence specific resonance assignments are annotated on peaks in **b-d**

rotor, was particularly useful to add assignments to loop 1 (residues 22–47), a region of general low peak intensity, and to define the β -strand edges. All obtained resonance assignments are annotated in Fig. 2b and c. Note the assigned proline residues, marked in red in Fig. 2c, that are unavailable from amide proton based assignment spectra. A representative strip plot for the assignments of residues 83 to 87 is shown in Figure S1. The amide $^1\text{H}^{\text{N}}$ and ^{15}N assignments were further cross-checked using a 3D NNH spectrum based on proton-proton BASS-SD mixing (Jain 2017). We found that for β -strands, the transfer to neighboring amide protons was particularly efficient using this technique. The assigned $^{13}\text{C}\alpha$ - $^1\text{H}\alpha$ pairs additionally provided a starting point to the analysis of a 3D CCH-TOCSY and a 4D HCCH-TOCSY spectra, which allowed the assignment of the majority of the sidechain aliphatic ^{13}C and ^1H resonances (Stanek 2016). We did not record additional spectra to assign the aromatic ring resonances.

The degree of protein folding in the extracellular domain of OmpW proteins is highly dependent on the experimental conditions and showed discrepancies between previously published X-ray and solution NMR studies of OmpW and OprG.

Analysis of the chemical shifts towards the secondary structure of AlkL revealed 13 β -strands and one short α -helix (Fig. 3). The positions of the β -strands are in good agreement with the X-ray structures of OmpW and OprG, proving that extensive folding of the extracellular domain is present in our DMPC preparation. The helix in AlkL is located in a different region compared to the other two proteins.

In conclusion, we have found experimental conditions that are close to the native environment of this outer membrane protein, and importantly also favor to a protein fold close the one previously observed via X-ray crystallography. We anticipate to gain new insight into the transport mechanism of the protein by applying further NMR measurements sensitive to dynamics and interactions with small molecules.

Accession Number

^1H , ^{13}C and ^{15}N backbone and side-chain chemical shifts of the outer membrane protein AlkL have been deposited in the BioMagResBank (<https://www.bmrb.wisc.edu>) under the accession number 34365.

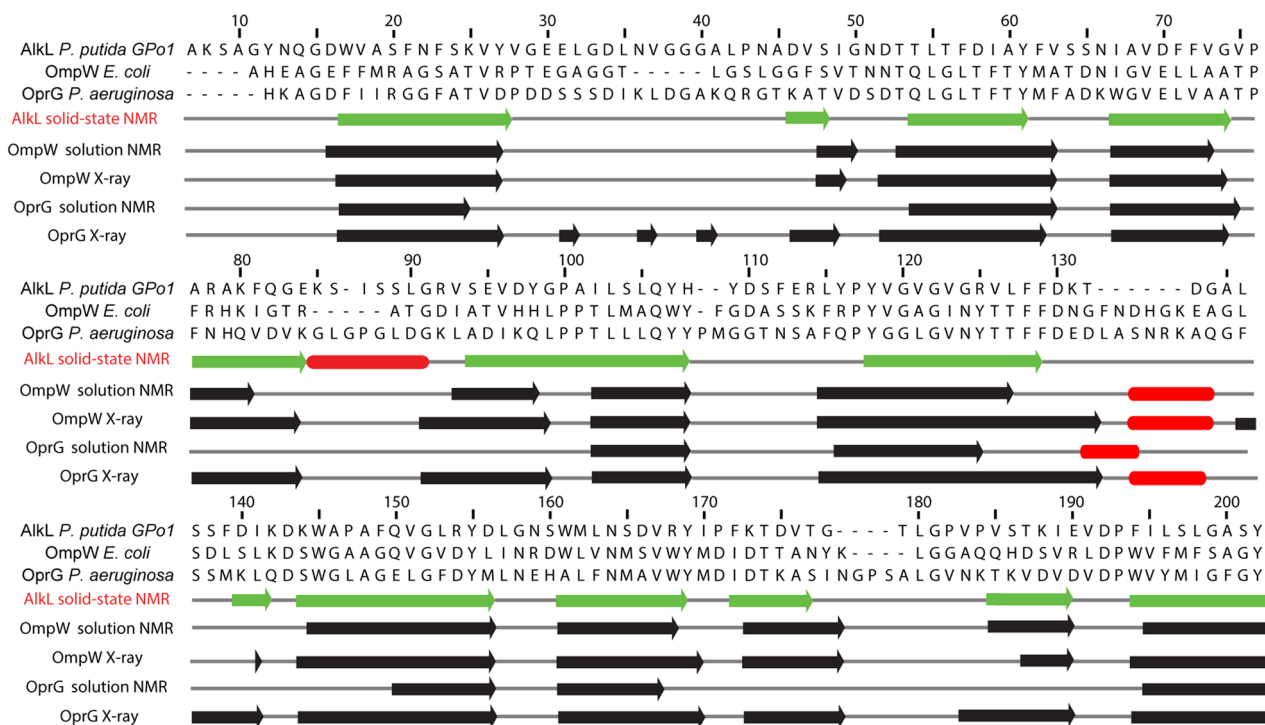


Fig. 3 Sequence alignment and secondary structure analysis of the proteins AlkL, OmpW and OprG. Backbone torsion angles were calculated from NMR chemical shifts using TALOS-N or directly

extracted from PDB files for X-ray crystal structures. β -strands are plotted as green or black arrows, and α -helices as red rounded rectangles

Acknowledgements We thank the cryoEM facility of the MPI-BPC for recording the negative stain images. The work was funded by the European Research Council (ERC-2015-CoG GA 648974 to GP), by the CNRS (IR-RMN FR3050), by the EC (Project iNext GA 653706), by the German Research Foundation (Emmy Noether Program Grant AN1316/1-1 and SFB803 Grant INST 186/794-3 to LBA) and by the German Federal Ministry of Education and Research (BMBF GA 031A178 to KC).

References

- Barbet-Massin E et al (2014) Rapid proton-detected NMR assignment for proteins with fast magic angle spinning. *J Am Chem Soc* 136(35):12489–12497
- Cala-de Paepe D, Stanek J, Jaudzems K, Tars K, Andreas LB, Pintacuda G (2017) Is protein deuteration beneficial for proton detected solid-state NMR at and above 100 kHz magic-angle spinning? *Solid State Nucl Magn Reson* 87:126–136
- Chen RR (2007) Permeability issues in whole-cell bioprocesses and cellular membrane engineering. *Appl Microbiol Biotechnol* 74(4):730–738
- Delaglio F, Grzesiek S, Vuister G, Zhu G, Pfeifer J, Bax A (1995) NMRPipe: a multidimensional spectral processing system based on UNIX pipes. *J Biomol NMR* 6(3):277–293
- Hong H, Patel DR, Tamm LK, van den Berg B (2006) The outer membrane protein OmpW forms an eight-stranded β -barrel with a hydrophobic channel. *J Biol Chem* 281(11):7568–7577
- Horst R, Stanczak P, Wüthrich K (2014) NMR polypeptide backbone conformation of the *E. coli* outer membrane protein W. *Structure* 22(8):1204–1209
- Hsieh S-C, Wang J-H, Lai Y-C, Su C-Y, Lee K-T (2018) Production of 1-dodecanol, 1-tetradecanol, and 1,12-dodecanediol through whole-cell biotransformation in *Escherichia coli*. *Appl Environ Microbiol* 84(4):e01806–e1817
- Jain MG et al (2017) Selective ^1H - ^1H distance restraints in fully protonated proteins by very fast magic-angle spinning solid-state NMR. *J Phys Chem Lett* 8(11):2399–2405
- Julsing MK, Schrewe M, Cornelissen S, Hermann I, Schmid A, Bühler B (2012) Outer membrane protein alkI boosts biocatalytic oxyfunctionalization of hydrophobic substrates in *Escherichia coli*. *Appl Environ Microbiol* 78(16):5724–5733
- Kucharska I, Seelheim P, Edrington T, Liang B, Tamm LK (2015) OprG harnesses the dynamics of its extracellular loops to transport small amino acids across the outer membrane of *Pseudomonas aeruginosa*. *Structure* 23(12):2234–2245
- Lakomek N-A, Frey L, Bibow S, Böckmann A, Riek R, Meier BH (2017) Proton-detected NMR spectroscopy of nanodisc-embedded membrane proteins: MAS solid-state vs solution-state methods. *J Phys Chem B* 121(32):7671–7680
- Lalli D et al (2017) Proton-based structural analysis of a heptahelical transmembrane protein in lipid bilayers. *J Am Chem Soc* 139(37):13006–13012
- Lee W, Tonelli M, Markley JL (2015) NMRFAM-SPARKY: enhanced software for biomolecular NMR spectroscopy. *Bioinformatics* 31(8):1325–1327
- Meng L, Li W, Bao M, Sun P (2018) Promoting the treatment of crude oil alkane pollution through the study of enzyme activity. *Int J Biol Macromol* 119:708–716
- Schubeis T, Le Marchand T, Andreas LB, Pintacuda G (2018) ^1H magic-angle spinning NMR evolves as a powerful new tool for membrane proteins. *J Magn Reson* 287:140–152

- Schwarzer TS, Hermann M, Krishnan S, Simmel FC, Castiglione K (2017) Preparative refolding of small monomeric outer membrane proteins. *Protein Expr Purif* 132:171–181
- Sharma K, Madhu PK, Agarwal V, Mote KR (2020) Simultaneous recording of intra- and inter-residue linking experiments for backbone assignments in proteins at MAS frequencies higher than 60 kHz. *J Biomol NMR*. <https://doi.org/10.1007/s10858-019-00292-y>
- Shen Y, Bax A (2013) Protein backbone and sidechain torsion angles predicted from NMR chemical shifts using artificial neural networks. *J Biomol NMR* 56(3):227–241
- Sievers F et al (2011) Fast, scalable generation of high-quality protein multiple sequence alignments using Clustal Omega. *Mol Syst Biol* 7(1):539
- Stanek J et al (2016) NMR spectroscopic assignment of backbone and side-chain protons in fully protonated proteins: microcrystals, sedimented assemblies, and amyloid fibrils. *Angew Chem Int Ed* 55(50):15504–15509
- Stanek J, Schubeis T, Paluch P, Güntert P, Andreas LB, Pintacuda G (2020) Automated backbone NMR resonance assignment of large proteins using redundant linking from a single simultaneous acquisition. *J Am Chem Soc* 142(12):5793–5799
- Touw DS, Patel DR, van den Berg B (2010) The crystal structure of OprG from *Pseudomonas aeruginosa*, a potential channel for transport of hydrophobic molecules across the outer membrane. *PLoS ONE* 5(11):e15016
- van Beilen JB, Funhoff EG (2007) Alkane hydroxylases involved in microbial alkane degradation. *Appl Microbiol Biotechnol* 74(1):13–21
- van Beilen JB, Neuenschwander M, Smits THM, Roth C, Balada SB, Witholt B (2002) Rubredoxins involved in alkane oxidation. *J Bacteriol* 184(6):1722–1732
- van Nuland YM, Eggink G, Weusthuis RA (2016) Application of AlkBGT and AlkL from *Pseudomonas putida* GPo1 for selective alkyl ester ω -oxyfunctionalization in *Escherichia coli*. *Appl Environ Microbiol* 82(13):3801–3807
- Vranken WF et al (2005) The CCPN data model for NMR spectroscopy: development of a software pipeline. *Proteins Struct Funct Genet* 59(4):687–696
- Xue K et al (2017) (2017) Limits of resolution and sensitivity of proton detected MAS solid-state NMR experiments at 111 kHz in deuterated and protonated proteins. *Sci Rep* 7(1):7444

Publisher's Note Springer Nature remains neutral with regard to jurisdictional claims in published maps and institutional affiliations.